Peer-reviewed version available at ChemEngineering 2018, 2, 33; doi:10.3390/chemengineering2030033

Article

Tio2 Assisted Photodegradation for low Substrate Concentrations and Transition Metal Electron Scavengers

Hassan Alsaud[1], Ahmed Abibat[1], R. Painter *[1], L. Sharpe[2], S.K. Hargrove[2]

[1] *Civil and Environmental Engineering, Tennessee State University, Nashville, TN 37209, USA*
[2] *Mechanical Engineering, Tennessee State University, Nashville, TN 37209, USA*

* *Correspondence: rpainter@tnstate.edu; Tel.:615-785-3901*

Abstract: *Some contaminants of emerging concern (CECs) are known to survive conventional wastewater treatment plants, which introduce them back to the environment and can potentially cycle up in drinking water supplies. This is especially concerning because of the inherent ability of some CECs to induce physiological effects in humans at very low doses. Advanced oxidation processes (AOPs) such as TiO2 based photocatalysis are of prominent interest for addressing CECs in aqueous environments. Natural water resources often contain dissolved metal cations concentrations in excess of targeted CEC concentrations. These cations may significantly, adversely impact degradation of CECs by scavenging TiO2 surface generated electrons. Consequently, simple pseudo first order or Langmuir-Hinshelwood kinetics are not sufficient for reactor design and process analysis in some scenarios. Rhodamine B dye and dissolved copper cations were studied as reaction surrogates to demonstrate that TiO_2 catalyzed degradation for very dilute solutions is very nearly completely due to homogeneous reaction with hydroxyl radicals and that in this scenario the hole trapping pathway has negligible impact. Chemical reaction kinetic studies were then carried out to develop a robust model for RB/metal reactions that is exact in the electron pathways for hydroxyl radical production and metal scavenging.*

Keywords: *TiO2; AOP; Photodegradation; Semiconductor based photocatalysis; reaction kinetics*

1. Introduction

There is a critical need for highly efficient new methods for the treatment of toxic and biologically persistent compounds that are not efficiently removed by conventional water treatment processes. This need has led to a compelling interest in semiconductor photooxidative degradation. Semiconductor based photocatalysis is an advanced oxidation process (AOP) that shows promise for removal of organic pollutants from water [1-4]. UV enhanced photocatalysis is also an effective method for disinfection similar in application to existing UV enhanced chlorination water disinfection processes [5-6].

Semiconductor photocatalysis can be more appealing than the more conventional chemical oxidation methods because semiconductors are inexpensive, nontoxic, and capable of extended use without substantial loss of photocatalytic activity [7]. The development of photocatalytic routes which rely on light as an energy source to drive chemical reactions under mild reaction conditions is highly desirable. Furthermore, semiconductor particles recovered by filtration or centrifugation or when immobilized in a fluidized bed reactor retain much of their native activity after repeated catalytic cycles. The term photodegradation is usually used to refer to complete oxidative mineralization; that is, the conversion of organic compounds to CO_2, H_2O, NO_3 or other oxides, halide ion, phosphate, etc. It has been widely demonstrated that the semiconductor TiO_2 is an effective photocatalysis for destruction of many organic contaminates. [8-12]. Halogenated substrates [13] have been decomposed successfully on irradiated semiconductor suspensions. When fluoroalkenes [14] or

fluoroaromatics [15] were exposed to an irradiated, air-saturated, aqueous suspension of anatase TiO_2 with UV light at room temperature, CO2 and HF were formed. The irradiation of a solution of chlorobenzene over TiO_2 similarly leads to complete mineralization to CO2, H2O, and HC1 [16]. Extensive studies of the photocatalytic degradation of organochlorine compounds have been undertaken because of their known carcinogenicity and because they are formed during water purification by chlorination. Perchloroethylenes, chloroethanes, chlorinated acetic acids, and chlorobenzenes, for example, are all readily mineralized on irradiated TiO_2 suspensions. Chloroform and carbon tetrachloride, other common contaminants of municipal water supplies are also mineralized [17-20] by UV irradiated TiO_2. The primary photochemical processes occurring upon irradiation of a semiconductor are now well established [21-23]. By definition, a semiconductor has band structure consisting of a series of energetically closed spaced energy levels associated with covalent bonding between atoms composing the crystallite (the valence band) and a second series of spatially diffuse, levels at higher energy and associated with conduction in the macromolecular crystallite (the conduction band). The magnitude of the fixed energy gap between the electronically populated valence band and the largely vacant conduction band governs the extent of thermal population of the conduction band. The band gap also defines the wavelength sensitivity of the semiconductor to irradiation. Unlike metals, semiconductors lack a continuum of inter-band states to assist the recombination of the electron-hole pair. This assures an electron-hole pair lifetime sufficiently long to allow them to participate in interfacial electron transfer [24]. Thus, the act of photoexcitation usually generates an electron-hole pair poised respectively at the conduction band and valence edges. The components of this activated pair, when transferred across the interface, are capable of reducing or oxidizing a surface-adsorbed substrate. Thus, an adsorbed electron donor can be oxidized by transferring an electron to a photo-generated hole on the surface, and an adsorbed acceptor can be reduced by accepting an electron from the surface. Hole trapping generates a cation radical, and electron trapping generates an anion radical. Many of the intermediates leading to mineralization of organic substrates on aqueous Ti02 suspensions are hydroxylated [25, 26]. Numerous studies have assumed competing roles for photo-generated OH radicals and for trapped holes in photocatalysis [27-31]. Reaction kinetic mechanisms have been proposed that suggest that at low substrate coverages associated with low concentrations, the photo-generated hydroxy radical diffuses into the homogeneous solution where it effects photooxidation, while it reacts at the surface when the substrate is present at higher coverages. This suggests that for low concentrations that the homogeneous OH radical production by the electron pathway is favored over the surface mediated hole pathway [32, 33]. Furthermore, the OH radical dye degradation pathway is also favored over the direct hole pathway in a similar fashion.

The class of contaminants targeted by our reactor design includes Pharmaceuticals and Personal Care Products (PPCP) and other toxic organic contaminants which are environmentally significant at low part per billion (ppb) levels [34]. Rhodamine B (RB) dye was used as a surrogate for our chemical reaction kinetics for contaminants at these levels. Rhodamine dye, a significant water contaminant in its own right, is easily measured at ng/L levels due to its fluorescence properties. The results below support our hypotheses that a mechanistic approach of the surrogate reaction kinetics based on the limiting nature of the kinetics for dilute solutions would provide a more robust model for the reaction kinetics than a simple curve fitting approach. In other words, it provides additional insight into the underlying complex interaction of reaction kinetics and adsorption equilibrium processes. This was especially important since our study also addressed the impact of transition metal cations typically present in drinking water supplies. These metal cations are known to scavenge electrons in competition with decontamination reactions [35].

2. Materials and Methods

Titanium (IV) oxide, anatase nano-powder with <25 nm particle size and 99.7% purity basis from Aldrich Chemistry was used as the photocatalytic material. Serial dilutions of 20% aqueous solution of Acros Organics' Rhodamine B and reagent grade Fisher Scientific copper sulfate were used for all experimental runs. Solutions of RB concentrations [D] ranging from 0.1 – 0.5 mg/L and copper cation concentration [Cu^{2+}] ranging from 0.0 – 0.5 mg/L with 0.02 mg/L suspended P-25 catalyst were irradiated in a cylindrical quartz glass bench scale reactor equipped with 365 nm LED lamps [36]. The inside diameter and reaction depth of the cylindrical reactor were 15 and 20 cm respectively and was equipped with 300, 3 mW 365 nm output lamps (NSHU5518) evenly distributed over its approximately 1000 cm^2 surface. The reaction system temperature was monitored and kept approximately constant at 298 K by fan cooling. Magnetic stirring was used to maintain homogeneity and catalyst suspension. The water supply was distillated and deionized. The reactor was initially stirred for 20 minutes without UV irradiation to reach the equilibrium adsorption/desorption of the dye on the catalyst. After the 20 minutes, the UV light was turned on and an initial sample was taken and subsequent samples were taken hourly. A Turner Designs fluorimeter model TD-700 was used to measure the concentration of the dye in each sample. The fluorimeter was calibrated every day with freshly prepared standards. Samples were diluted to remain in the linear range for the TD-700 for Rhodamine B of .001 to .100 mg/L [37].

3. Results

The detailed stoichiometric balances in Appendix A and application of the quasi-steady state assumption (QSSA) for all species leads to [35, 39]:

$$-r_D = k_{OH}[D] + k_1[D]\left(\left(\frac{k_3}{1+K_2[D]} + \frac{k_4}{1+K_2[D]}\right) * \frac{1}{1+K_6[Cu^{2+}]}\right) \quad (1)$$

where r_D is the dye degradation rate and K_2 and K_6 are adsorption equilibrium constants for the dye and copper cation respectively. The constants designated by lower case k's are chemical reaction rate constants for various intermediate species and defined below. This general equation can be simplified by inversion and neglecting the squared [D] terms to give

$$\frac{1}{r_D} = \left(\frac{1}{[D]} + K_2\right)\frac{(1+K_6[Cu^{2+}])}{(k_0+K_6k_7[Cu^{2+}])} \quad (2)$$

where $k_0 = k_{oh} + k_1 k_3 + k_1 k_4$ and $k_7 = k_{oh} + k_1k_3$.

The compound rate constants, k_1k_3 and k_1k_4, refer to the generation of $OH^{\bullet}$ by hole and electron pathways, respectively. A further simplification is obtained by setting [Cu^{2+}] equal to zero

$$\frac{1}{r_{D_0}} = \left(\frac{1}{[D]} + K_2\right)\frac{1}{k_0} \quad (3)$$

where r_{D_0} is the initial dye degradation reaction rate.

3.1. Determining k_0 and K_2

Eq. 3 represents a linear relationship between the inverse of the initial reaction rate $1/r_{D0}$ and the inverse of the dye concentration 1/ [D] with slope 1/ k_0 and intercept K_2/k_0 for the case where $[Cu^{2+}] = 0$. A series of experimental runs were then conducted with $[Cu^{2+}] = 0$ and for various initial values of [D] ranging from 0.1 to 0.5 mg/l. The initial reaction rates for these runs was fit to Equation (3) as shown in Figure 1. The slope and intercept of the

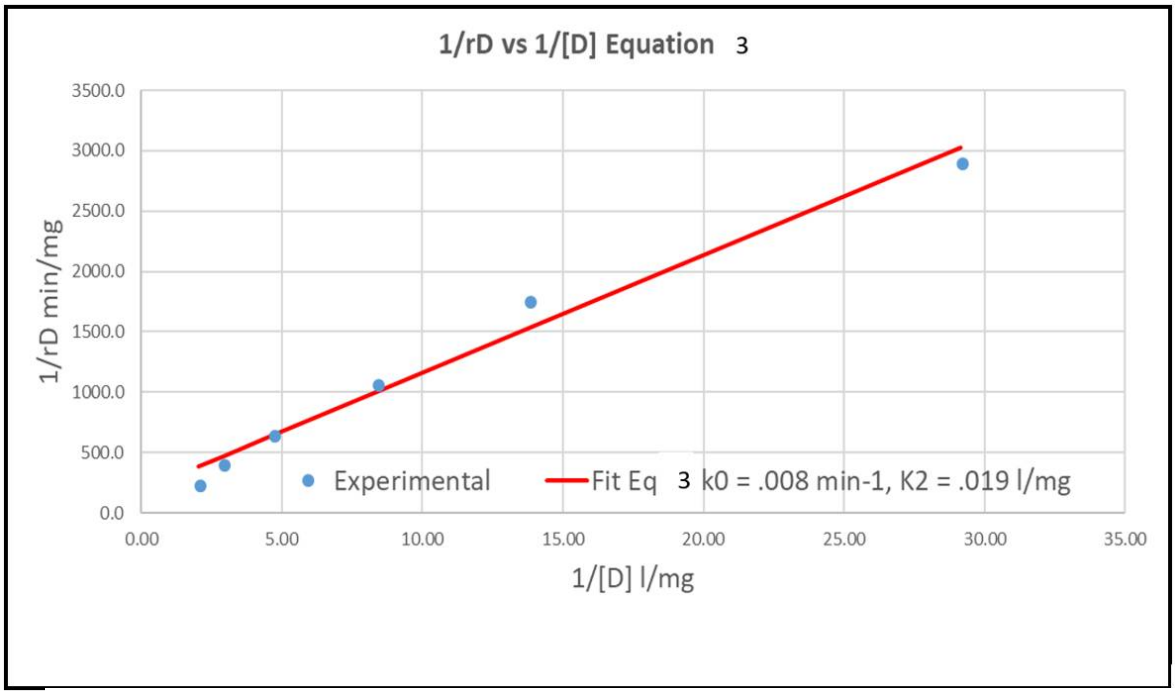

Figure 1 Linear Regression of Equation 3 giving k_0 = 0.008 min^{-1} and K_2 = 0.019 l mg^{-1}.

plot gave k_0 = 0.008 min^{-1} and K_2 = 0.019 l mg^{-1}.

Preprints (www.preprints.org) | NOT PEER-REVIEWED | Posted: 6 June 2018 doi:10.20944/preprints201806.0094.v1

Peer-reviewed version available at ChemEngineering 2018, 2, 33; doi:10.3390/chemengineering2030033

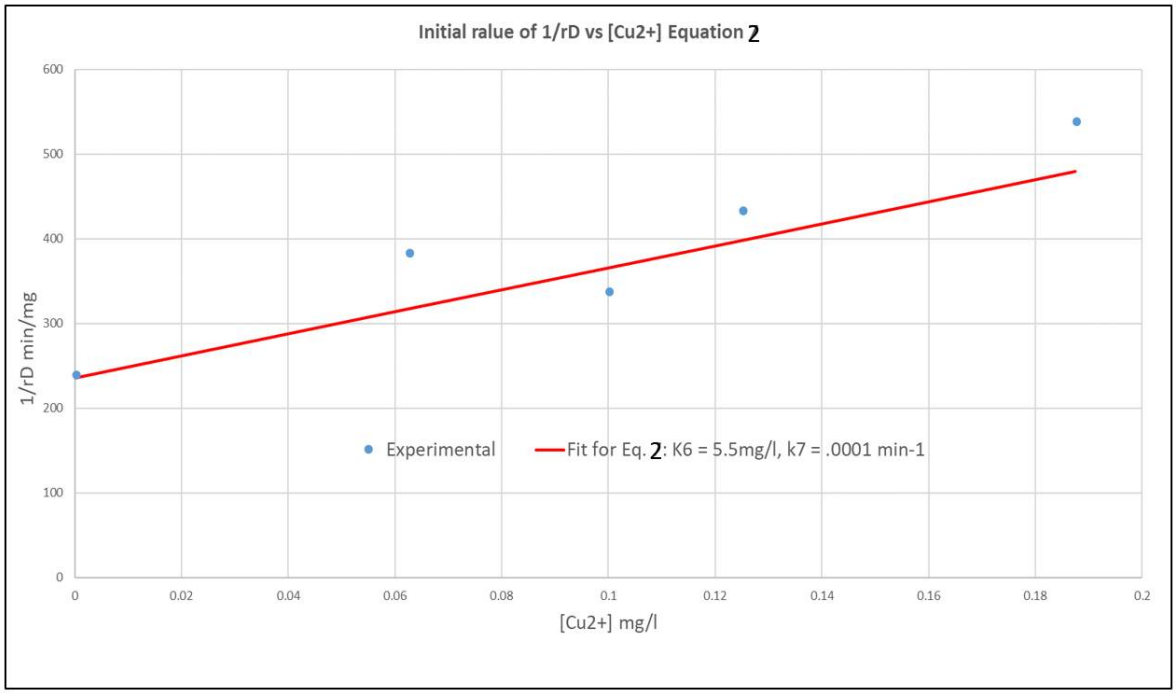

Figure 2 Non-Linear Regression giving k7 = 0.0008 min^{-1} and K_6= 5.50 L/mg

3.2 Determining k_7 and K_6

A series of runs was conducted with the initial concentration of the dye [D] at .500 mg/L and for [Cu^{2+}] ranging from 0.0625 to 0.5 mg/L. Using the values of k_0 and K_2 obtained above. The data was regressed non-linearly to fit Equation 2 as shown in Figure 2. The resulting values of K6 and k7 were 5.5 l/mg and 0.0001 /min respectively.

3.3 Validation of the model

Based on these results, neglecting k_7 results in approximately 10.0 percent error relative to k_0 which is well within the contingencies for engineering design. Several other simplifications occur in Equation 4 under this approximation as $k_{0h} = k_3 = 0$ and $k_0 = k_1 k_4$. Equation 4 becomes

$$-r_D = -\frac{d[D]}{dt} = \frac{k_0[D]}{(1+K_2[D])\,(1+K_6[Cu^{2+}])} \qquad (4)$$

which is first order in [D] and limited by [D] and [Cu^{2+}] surface adsorption. In Figure 3 the model (Equation 4) was verified for [D] 500 mg/L and for [Cu^{2+}] 0.0625, 0.1875 and 0.3750 mg/L.

Preprints (www.preprints.org) | NOT PEER-REVIEWED | Posted: 6 June 2018 doi:10.20944/preprints201806.0094.v1

Peer-reviewed version available at ChemEngineering 2018, 2, 33; doi:10.3390/chemengineering2030033

4. Discussion

The reaction between the substrate and photo-generated oxidant can occur while both species are adsorbed, with an adsorbed substrate and a free oxidant, with a bound oxidant and a free substrate, or with both the oxidant and substrate freely dissolved. Unfortunately, an experimental distinction between these pathways, based on chemical kinetics alone (fitting reaction data to Eq. 1), is not possible. Alternatively, a purely

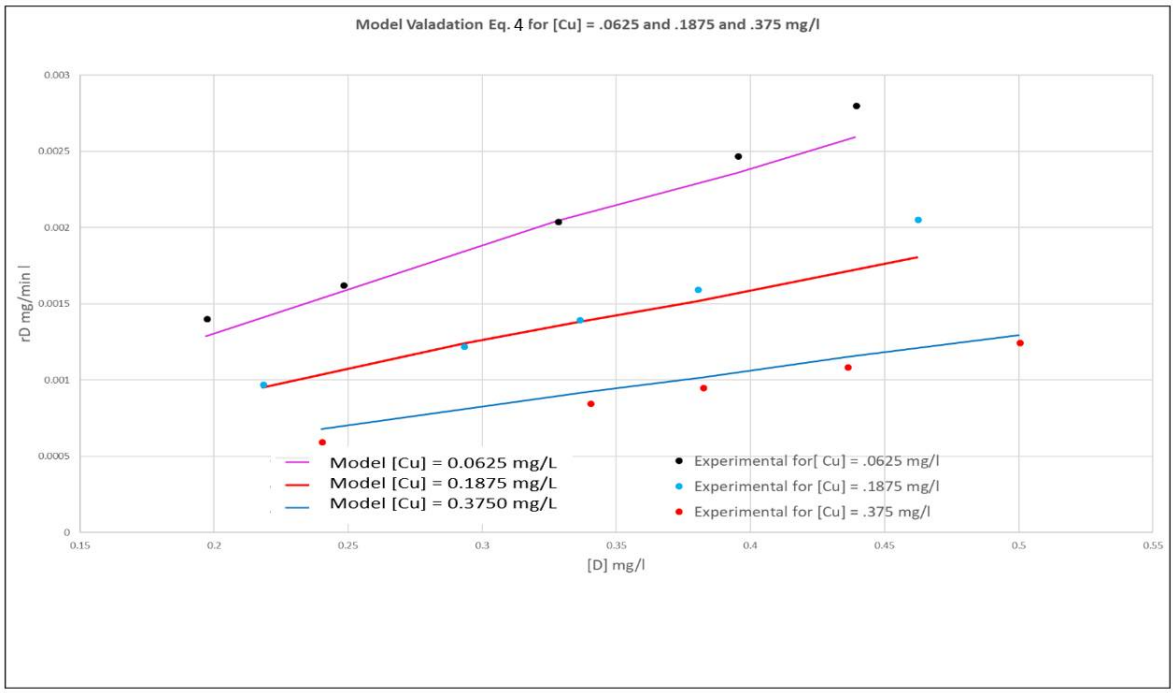

Figure 3: Model (Equation 4) Validation for $[Cu^{2+}]$ *0.0625, 0.1875, 0.03750 mg/L*

chemical kinetics fit does not provide insights into the mass transfer mechanisms associated with the observed rates that are required for reactor design. The Langmuir-Hinshelwood (LH) kinetics model approach avoids the necessity for a complex mathematical formulation of surface binding but it has severe inherent limitations. On the other hand, a rigorous formulation would require several intermediate parameters that cannot be determined experimentally. Our model addresses this by providing a robust parametrization of Eq. 1 by capitalizing on the preference of the electron pathway for dilute solutions with low surface substrate coverage. Several intermediate parameters associated with the hole pathway were shown to be practically zero which allowed the complete experimental determination of electron pathway parameters. The electron pathway for degradation shown by the green arrows in Scheme 1 is an exact mechanism for the limiting conditions.

The —S terms in Scheme 1 designate species adsorbed to the catalyst surface.

Preprints (www.preprints.org) | NOT PEER-REVIEWED | Posted: 6 June 2018 doi:10.20944/preprints201806.0094.v1

Peer-reviewed version available at ChemEngineering 2018, 2, 33; doi:10.3390/chemengineering2030033

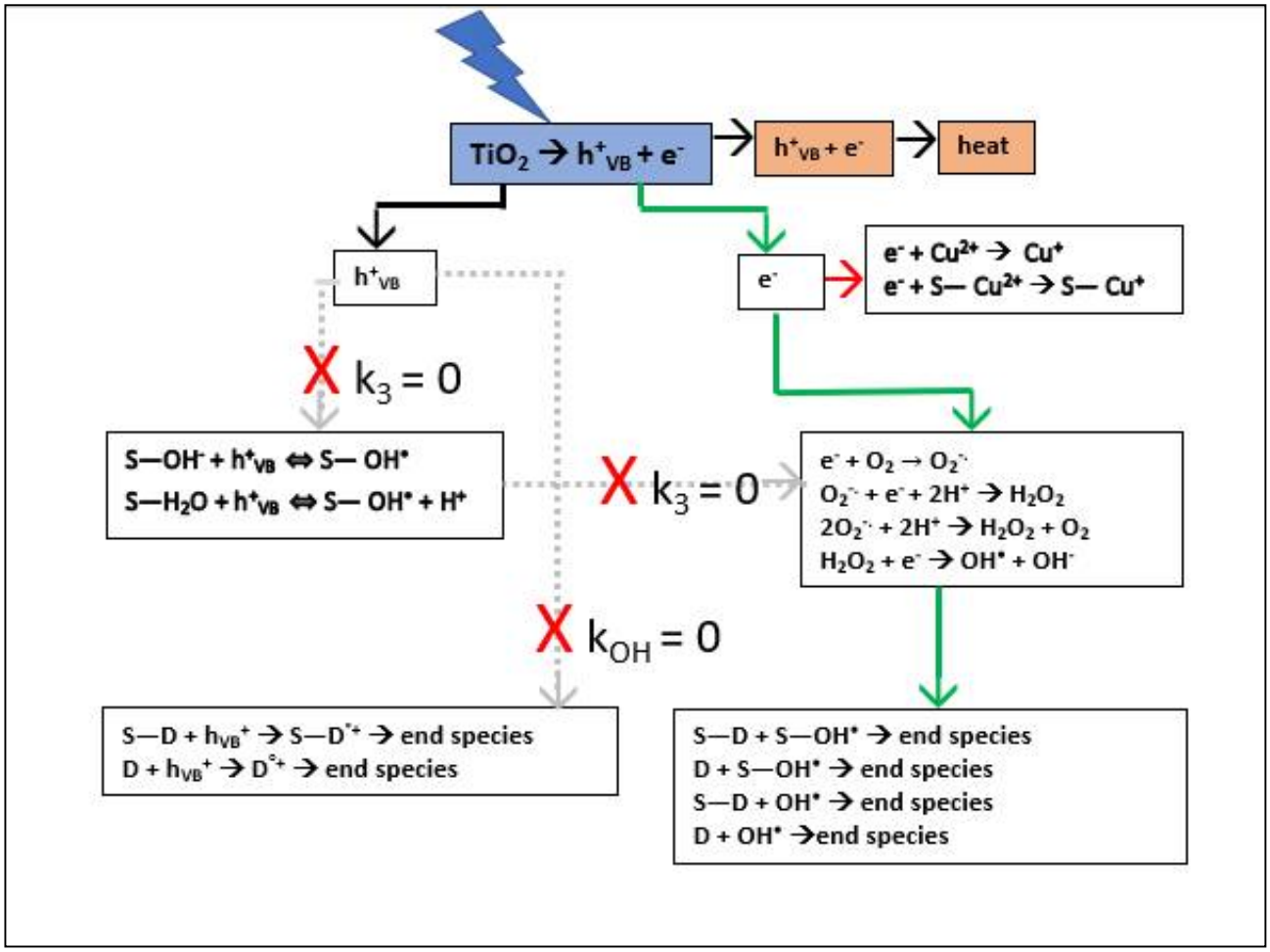

Scheme 1 Simplified Electron Pathway ($k_7 = k_3 = k_{OH} = 0$) Kinetics for Low Concentrations with the Presence of Electron Scavengers

References

(1) Ibhadon, A.O.; Fitzpatrick, P. Heterogeneous Photocatalysis: Recent Advances and Applications. *Catalysts***2013**, *3*, 189-218

(2) Salimi M, Esrafili A, Gholami M, Jonidi Jafari A, Rezaei Kalantary R, Farzadkia

(3) Kermani M, Sobhi HR, Contaminants of emerging concern: a review of new approach in AOP technologies. *Environ Monit Assess*. 2017 Aug;189(8):414. doi: 10.1007/s10661-017-6097-x. Epub 2017 Jul 24.

(4) Lazar M., Varghese S., Nair S. Photocatalytic Water Treatment by Titanium Dioxide: Recent Updates. *Catalysts*. 2012; 2(4):572-601.

(5) Mills, A., LeHunte, S. An overview of semiconductor photocatalysis. J. Photochem. Photobiol. A 1997, 108, 1–35.

(6) Sunada, K.; Watanabe, T.; Hashimoto, K. Studies on photo-killing of bacteria on TiO_2 thin film. *J. Photochem. Photobiol. A* 2003, *156*, 227–233.

(7) Paleologou, A.; Marakas, H.; Xekoukoulotakis, N.P.; Moya, A.; Vergara, Y.; Kalogerakis, N.; Gikas, P.; Mantzavinos, D. Disinfection of water and wastewater by TiO_2 photocatalysis, sonolysis and UV-C irradiation. *Catal. Today* 2007, *129*, 136–142.

(8) Khairy, M., Zakaria, W. Effect of metal-doping of TiO_2 nanoparticles on their photocatalytic activities toward removal of organic dyes. *Egyptian Journal of Petroleum*. Volume 23, Issue 4, December 2014, Pages 419-426

(9) Chan, P., El-Din, M., Bolton, J. Water Res., 46 (2012), pp. 5672-5682
(10) Oller, I., Malato, S., Sánchez-Pérez, J. Sci. Total Environ., 409 (2011), pp. 4141-4166
(11) V.K. Sharma, T.M. Triantis, M.G. Antoniou, X. He, M. Pelaez, C. Han, W. Song, K.E. O'Shea, A.A. de la Cruz, T. Kaloudis, A. Hiskia, D.D. Dionysiou Sep. Purif. Technol., 91 (2012), pp. 3-17
(12) S. Cortez, P. Teixeira, R. Oliveira, M. Mota J. Environ. Manage., 92 (2011), pp. 749-755
(13) Blake, D. *Bibliography of Work on the Heterogeneous Photocatalytic Removal of Hazardous Compounds from Water and Air*; National Renewable Energy Laboratory: Denver, CO, USA, 2001; pp. 1–158.
(14) Hisanaga, T.; Harada, K.; Tanaka, K. *J. Photochem. Photobiol. A: Chem.* **1990**, 56,113.
(15) Ohtani, B.; Ueda, Y.; Nishimoto, S.; Kagiya, T.; Hachisuka, H. *J. Chem. Soc., Perkin Trans. 2* **1990**, 1955.
(16) Minero, C.; Aliberti, C.; Pelizzetti, E.; Terzian, R.; Serpone, N. *Langmuir* **1991**, 7, 928.
(17) Matthews, R. W. *J. Catal.* **1986**, 97, 565.
(18) Pruden, A. L.; Ollis, D. F. *J. Catal*. **1983**,82,404.
(19) Ollis, D. F.; Hsiao, C. Y.; Budiman, L.; Lee, C. L. J. *Catal.* **1984**,88,89.
(20) Bahnemann, D. W.; Monig, J.; Chapman, R. *J. Phys. Chem*. **1987**, 91, 3782.
(21) Serphone, N., Pelizzetti, E., Eds. *Photocatalysis – Fundamentals and Applications;* Wiley Interscience: New York, 1989.
(22) Fox, M. A. *Acc. Chem. Res.* **1983**,16, 314.
(23) Bard, A. *J. Science **1980***, 207, 139.
(24) Nosaka, Y.; Fox, M. A. J. Phys. Chem. 1988,92,1893.
(25) Pichat, P. *J. Photochem. Photobiol. A: Chem*. **1991**, 58, 99.
(26) Sclafani, A.; Palmisano, L.; Schiavello, M. *J. Phys. Chem.* **1990**, 94, 829.
(27) Fox, M. Dulay,M., Hetrogeneous Photocatalysis, *Chem. Rev.***1993,** 93, 341-357.
(28) Brezova, V.; Stasko, A.; Lapcik, L., Jr. J. *Photochem. Photobiol. A: Chem*. **1991**, 59,115.
(29) Howe, R. F.; Gratzel, M. *J. Phys. Chem.* **1987**, 91, 3906.
(30) Soria, J.; Conesa, J. C.; Auguliaro, V.; Palmisano, L.; Schiavello, M.; Sclafani, A. *J. Phys. Chem. **1991***, 95, 274.
(31) Tanaka, K.; White, J. M. *J. Phys. Chem.* **1982**, 86, 4708.
(32) Peral, J.; Casado, J.; Domenech, J. *J. Photochem. Photobiol. A; Chem.* **1988,** 44, 209.
(33) Turchi, C. S.; Ollis, D. F. *J. Catal.* **1990**,122, 178.
(34) Weir, A.; Westerhoff, P.; Fabricus, L.; Hristovski, K.; von Goetz, N. Titanium dioxide nanoparticles in food and personal care products. *Environ. Sci. Technol.***2012**, *46*, 2242–2250.
(35) Aarthi, T;Giridhar Madras,G. *Ind. Eng. Chem. Res.*, **2007**, *46* (1), pp 7–14
(36) Chuncheng Chen, Xiangzhong Li, Wanhong Ma, and Jincai Zhao, Effect of Transition Metal Ions on the TiO_2-Assisted Photodegradation of Dyes under Visible Irradiation: A Probe for the Interfacial Electron Transfer Process and Reaction Mechanism, *J. Phys. Chem. B, **2002**, 106 (2), pp 318–324*
(37) Yu, L.; Achari, G.; Langford, C.H. Photocatalytic degradation of 2,4-D with a LED based photoreactor. In Proceedings of 12th International Environmental Specialty Conference, Edmonton, Canada, 12–16 March 2012.
(38) http://www.comm-tec.com/Prods/mfgs/TurnerDesigns/application_notes_pdf/TD-700%20FAQ.pdf

270 (39) Nagaveni, K., Sivalingam, J., M. S. Hegde, M., and Giridhar, M. Photocatalytic
271 Degradation of Organic Compounds over Combustion-Synthesized Nano-TiO_2,
272 *Environ. Sci. Technol.*, **2004**, *38* (5), pp 1600–1604,**DOI:** 10.1021/es034696i
273 (40)